A Theoretical and Experimental Examination of the Bubble Jet Energy Window

Robert Cornell
Lexmark International, Inc., Lexington, Kentucky

Abstract

It is well known in the industry that thermal ink jet has a characteristic response to input energy. The response has a steep rise followed by a relatively flat portion. A 2D finite element heat transfer model was created to study the transient temperature response in the vicinity of the active heater. The model explains the shape of the characteristic performance curve. For consistent jetting performance, the input energy must be above the knee of the curve, for all circuit tolerances. However, overdriving the heaters will degrade their life. This paper also discusses the thermal effect of overdriving the heaters and the resultant degradation of heater chip life.

Introduction

The objective of the print head drive circuit is to deliver a well defined dose of electrical energy to the heater chip for conversion into thermal energy. This thermal energy heats a thin layer of ink at the surface of the chip. The heat affected zone is only a few microns thick. During the fire pulse, ink adjacent to the heater rapidly superheats, and boiling occurs. Vapor bubble growth is fed by thermal energy in the superheated ink layer. As the vapor bubble grows, it imparts momentum to the surrounding fluid, pushing ink out of the nozzle. The physics of this printing process has been reported by many investigators.

Thermal ink jet print heads have a characteristic response to input energy. Below a certain threshold, the thermal energy is insufficient to heat the ink to the film boiling temperature, and no bubble is formed. However, when input energy exceeds the threshold, the ink layer above the heater explodes into vapor. Bubble pressures can exceed 100 atmospheres.

Because water vapor has low diffusivity, the ink is thermally disconnected from the heater surface once the bubble begins to grow. For this reason, it is expected that the response curve will be flat for input energies above the threshold. This is illustrated in Figure 1. The data was taken on print heads developed and manufactured by Lexmark for the IBM 4076 printer. Figure 1 illustrates the shape of the response curve for several pulse widths. For a given input energy, 4.0 µs pulse widths produce smaller droplets than 3.2 µs pulse widths. This property and the shape of the drop mass response curves can be explained by considering the effective heater length. The effective heater length can be determined by studying the thermal response of the firing chamber.

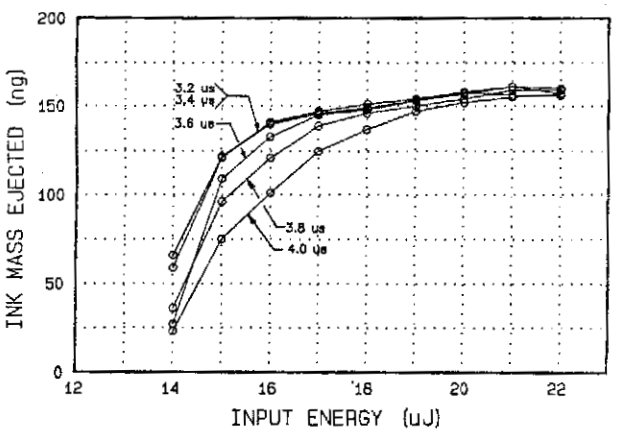

Figure 1. Characteristic Response Curves

Thermal Response

During each fire pulse, the active heater region is exposed to several hundred megawatts per square meter. This monstrous power density produces extraordinary temperature transients in the thin film layers. When power is applied, the heater temperature climbs at a rate exceeding 100 million °C per second. Because this heating rate makes direct temperature measurement difficult, a two dimensional finite element analysis (FEA) model was created to study the unsteady state heat conduction in the domain of the heater.

Simulation Model

Transient heat transfer simulations can be performed by several commercially available, general purpose FEA packages. However, coupling transient heat transfer with phase change, bubble growth and liquid motion is a very specialized application and not in the domain of general

Originally published in *Proc. of IS&T's 47th Annual Conference: The Physics and Chemistry of Imaging Systems,* May 15-20, 1994, Rochester, New York.

purpose FEA packages. For this reason, an application specific FEA model was created in the *APL* program language.

After the model is loaded with the appropriate firing chamber geometry, drive conditions and material properties, the program automatically generates nodes and elements. Because the heater is symmetrical, only half of the domain is meshed. The model uses a variety of numerical techniques.[1] A bandwidth technique is used to minimize storage requirements. Gaussian elimination, forward decomposition and backward substitution are used to minimize computation time. And Galerkin's method is used to maximize stability of the transient solution. The phase change-bubble growth portion of the model is not discussed in this paper.

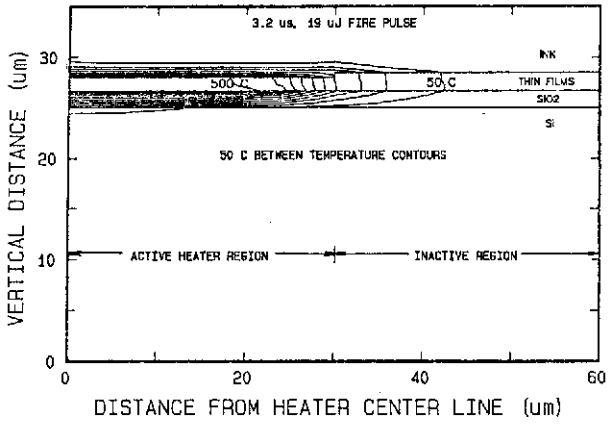

Figure 2. Thermal Simulation: 3.2 µs, 19 µJ Pulse

Figure 2 shows the simulated temperature contours for a 3.2 µs fire pulse. The domain of interest is the silicon substrate, silicon dioxide thermal barrier, hafnium diboride heater, aluminum wiring, silicon nitride-silicon carbide-tantalum overcoats, and ink. Power is applied to the HfB_2 elements in the active heater region. The inactive heater region contains the aluminum wiring. Figure 3 shows the same structure and input energy, but the pulse width has been increased to 4.0 µs.

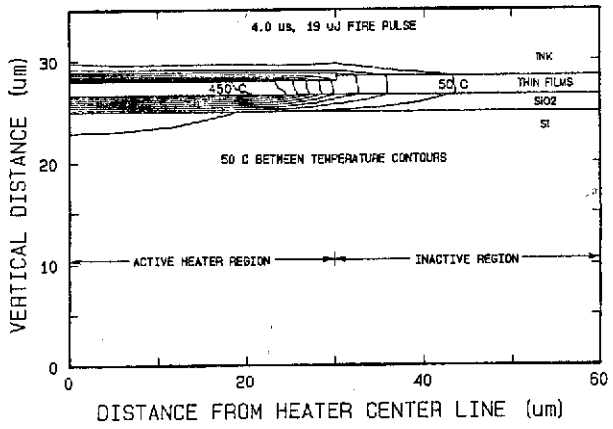

Figure 3. Thermal Simulation: 4.0 µs, 19 µJ Pulse

Since the SiO_2 layer was designed to insulate the substrate during 3.4 µs fire pulses, longer pulses allow a portion of the thermal energy to diffuse into the substrate. Even though a thick thermal barrier insulates the substrate, ensuring the fire pulse energy flows into the ink, it is advantageous to make the SiO_2 layer as thin as possible. A properly sized thermal barrier will insulate the substrate during the fire pulse, but allow thermal energy to diffuse into the Si between fires. For longer pulse widths, the structure under study will have lower temperatures at the heater surface because a portion of the input energy is spent in the substrate prior to bubble nucleation.

The model was used to simulate the effect of pulse width and input energy. The resultant surface node temperatures are shown in Figures 4 and 5. The central portion of the active heater has a constant temperature. However, the adjacent inactive region, containing the aluminum wiring, is relatively cool. Only 15 microns of the inactive region experience a temperature rise during the fire pulse. The edge of the active heater is well below the nucleation temperature.

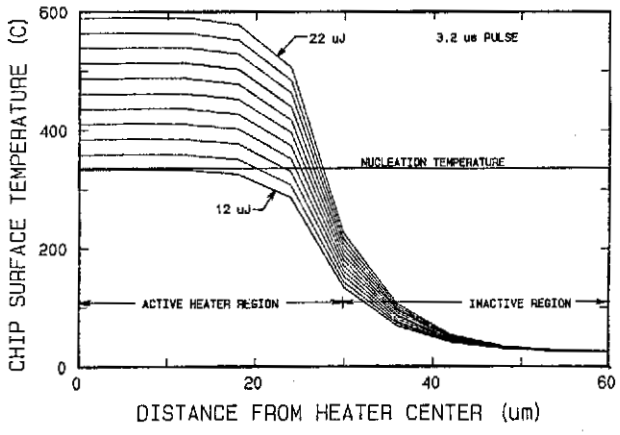

Figure 4. Surface Temperature: 3.2 µs Pulse

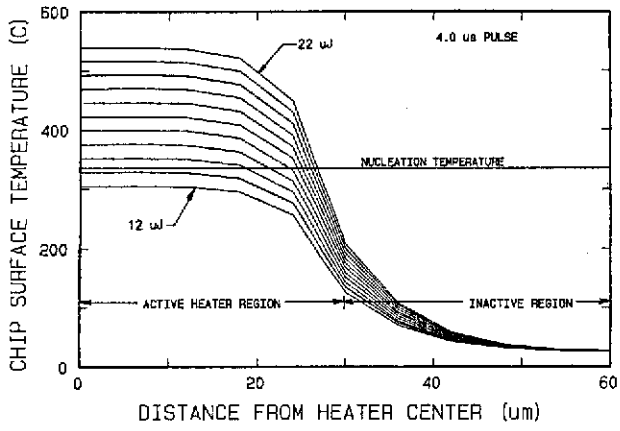

Figure 5. Surface Temperature: 4.0 µs Pulse

Nucleation Temperature

Classical thermodynamics dictates a critical point for water: 374 °C, 218 atmospheres. Beyond this *(T,P)*

water cannot exist as a liquid. Ink in the firing chamber is at one atmosphere. At this pressure, nucleate boiling can occur with as little as 10°C of superheat[2]. However, ink jet printing does not operate in the nucleate boiling regime. It is a film boiling process[3]. The literature varies on the nucleation temperature of ink-jet film boiling.[4,5,6,7,8,9,10] Recently, Runge[11] investigated this problem and published empirical results relating ink jet nucleation temperature to the temperature gradient at the ink-heater interface. For the firing chamber in this application, the temperature gradient is approximately 620 K/μm at the heater-ink interface. This gradient drives the nucleation temperature to 329°C.

Effective Heater Length

The horizontal lines in Figures 4 and 5 are drawn at 329°C. The heater region that reaches this temperature will contribute to film boiling. This is the effective heater length. Because of the transition zone between hot and cold regions, the effective heater length is not as large as the physical heater pattern. The effective heater length is zero until the input energy is sufficient to drive the ink-heater interface to the nucleation temperature. Figures 4 and 5 show that above this threshold, increasing input energy will not have a linear effect. The length of the heater exceeding the nucleation temperature will rapidly increase, then reach a point of diminishing return. The simulation results are summarized in Figure 6. This plot shows how the effective heater length varies with input energy and pulse width. The shape of the curves in Figure 6, as well as their relative positioning, is similar to the shape of the experimental response curves of Figure 1.

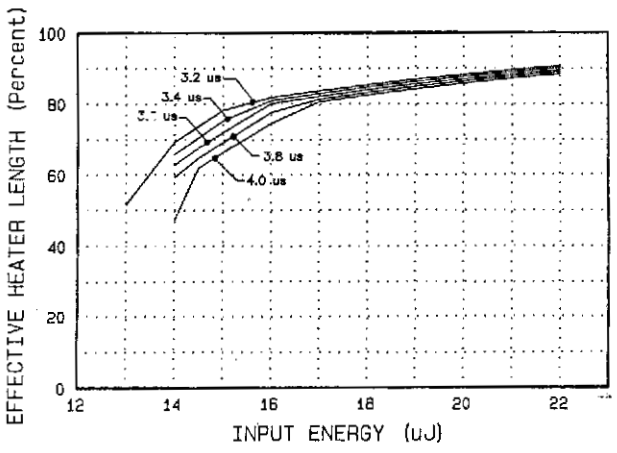

Figure 6. Effective Heater Length

Input Energy and Heater Life

It is important that the energy delivered to the heater exceeds the knee of the characteristic response curve, for all circuit tolerances. There are also practical limitations on how far the energy window is allowed to extend to the right. The reason for the lower limit is obvious. At low energies, the print head will jet poorly, if at all. The upper limit is set because higher input energy drives higher heater temperatures. Higher temperatures require more time to cool between fires, accelerate kogation,[12] and accelerate heater failures.

Heater Life and Temperature

The print head is a disposable supply item. Once the ink reservoir is depleted, the print head is discarded. This ensures high reliability. Unless a defect causes infant mortality, heater chips do not fail during the life of the print head. During development, thousands of print heads were tested to verify this. But to understand the life time characteristics of the heater chip, reliability statistics dictates that some population must be tested to failure. To this end, a designed experiment was performed. Several hundred print heads were tested to failure at various energy levels. Because chip life is much greater than the reservoir capacity, these heads were specially assembled with the necessary plumbing to continually feed ink from an external tank.

Given enough time, any component can be tested to failure. During this long term life test, it was observed that chips generally fail in the vicinity of the active heaters, when they do fail. Because the heaters experience millions of heating-cooling cycles, it is reasonable to assume that chip life is a function of temperature. The Arrhenius equation[13] is commonly used to model acceleration of component failures due to increased temperature.

$$N_{50} = Ae^{\frac{\Delta H}{kT}} \quad (1)$$

N_{50}=average life
A=constant
ΔH=activation energy (eV)
k=Boltzmann's constant
T=component temperature (k)

In this application, the temperature governing heater life is a function of the thin film response to peak power and the bulk chip response to average power.

Monte Carlo analysis of the circuit components suggest that input energy will have a normal distribution with a mean (μ) and standard deviation (σ). The window tested in this experiment extended from 3% less energy than (μ - 6σ), to 25% more energy than (μ + 6σ), greatly exceeding any statistically probable condition.

Analysis of the long term life test data indicated that failures could be modeled by the lognormal distribution. Also, the data followed the Arrhenius equation, with a high degree of fit. The coefficient of determination was 0.9. In other words the empirical model developed from the data could account for 90% of the variability in the data. Equally important, it was also found that the lognormal distribution shape factor remained constant. Only the scale factor shifted with temperature. Further indication that the degradation process obeys an Arrhenius model. Figure 7 illustrates the generalized results of this test.

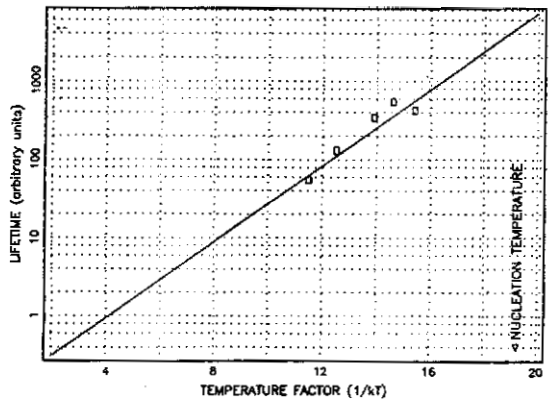

Figure 7. Arrhenius Model Results

Conclusion

The shape of the characteristic performance curve can be explained by studying the thermal response of the firing chamber. Greatly increasing the input energy beyond the knee of the curve will not have a significant impact on the effective heater length, and the characteristic response curve will stay relatively flat. Thermal simulations closely mimic the experimental results.

The heater chip failure mode follows the lognormal distribution. And the acceleration of failure due to temperature obeys the Arrhenius model.

References

1. L. J. Segerlind, *Applied Finite Element Analysis*, John Wiley and Sons, New York, 1976.
2. M . S. Plesset, and S. A. Zwick, "The Growth of Vapor Bubbles in Superheated Liquids", *J. Appl. Phys.*, **25:** 493, (1954).
3. A. Asai, S. Hirasawa, and I. Endo, "Bubble Generation Mechanism in the Bubble Jet Recording Process", *J. Im. Tech*., **14:** 120, (1988).
4. R. R. Allen, J. D. Meyer and W. R. Knight, "Thermodynamics and Hydrodynamics of Thermal Ink Jets", *Hewlett Packard J*., **36:** 21 (1985).
5. M. Tirumala, and F. C. Lee, "Thermal Analysis of Thermal Ink-Jet Heater Structure", *SID 88 Digest*., 268, (1988).
6. A. Asai, T. Hara, and I. Endo, "One Dimensional Model of Bubble Growth and Liquid Flow in Bubble Jet Printers", *Japanese J. Appl. Phys*., **26**: 1794, (1987).
7. A. Mirfakhraee, "An Analysis of the Growth and Collapse of Vapor Bubbles in Ink Jet Printers", *IBM Research Division, Report # RJ 6823*, (1989).
8. J. Poppel, "Measurement of Temperature Gradients at t he Heater of a Bubble Jet by Detection of the Nucleation", *SID 89 Digest*, **176**, (1989).
9. W. Runge, "One Dimensional Simulation of a Phase Change Cycle in Thermal Ink-Jet Printers", *SID 87 Digest*, **189**, (1987).
10. P. A. Torpey, "Prevention of Air Ingestion in a Thermal Ink Jet Device", *Proc. 4th Int. Cong. Adv. Non-Impact Printing Tech.*, **275**, (1988).
11. W. Runge, "Nucleation in Thermal Ink-Jet Printers", *Proc. 8th Int. Cong. Adv. Non-Impact Printing Tech*., **299**, (1992).
12. L.S. Chang, "Mechanisms of Failure of Thermal Ink-Jet Thin Film Devices Under Stressed Conditions", *Proc. SID*, **30**: 57, (1989).
13. P. Tobias, and D. Trindade, *Applied Reliability*, Van Nostrand, New York, 1986.